Redox Biology 62 (2023) 102636

Contents lists available at ScienceDirect

Redox Biology

journal homepage: www.elsevier.com/locate/redox

Release of hepatic xanthine oxidase (XO) to the circulation is protective in intravascular hemolytic crisis

Heidi M. Schmidt [a], Evan R. DeVallance [b,c], Sara E. Lewis [c], Katherine C. Wood [d], Gowtham K. Annarapu [d], Mara Carreño [a,1], Scott A. Hahn [d], Madison Seman [c], Brooke A. Maxwell [c], Emily A. Hileman [c], Julia Z. Xu [d,e], Murugesan Velayutham [h], Werner J. Geldenhuys [f,g], Dario A. Vitturi [a,d,1], Sruti Shiva [a,d], Eric E. Kelley [c,*], Adam C. Straub [a,d,**]

[a] Department of Pharmacology and Chemical Biology, University of Pittsburgh, Pittsburgh, PA, USA
[b] Center for Inhalation Toxicology, West Virginia University School of Medicine, Morgantown, WV, USA
[c] Department of Physiology and Pharmacology, Health Sciences Center, West Virginia University, Morgantown, WV, USA
[d] Heart, Lung, Blood and Vascular Medicine Institute, University of Pittsburgh, Pittsburgh, PA, USA
[e] Division of Hematology /Oncology, Department of Medicine, University of Pittsburgh, Pittsburgh, PA, USA
[f] Department of Pharmaceutical Sciences, School of Pharmacy, West Virginia University, Morgantown, WV, USA
[g] Department of Neuroscience, School of Medicine, West Virginia University, Morgantown, WV, USA
[h] Department of Biochemistry, West Virginia University School of Medicine, USA

ARTICLE INFO

Keywords:
Xanthine oxidase
Sickle cell disease
Hemolysis
Hemin
Hemoglobin
Oxidants

ABSTRACT

Xanthine oxidase (XO) catalyzes the catabolism of hypoxanthine to xanthine and xanthine to uric acid, generating oxidants as a byproduct. Importantly, XO activity is elevated in numerous hemolytic conditions including sickle cell disease (SCD); however, the role of XO in this context has not been elucidated. Whereas long-standing dogma suggests elevated levels of XO in the vascular compartment contribute to vascular pathology via increased oxidant production, herein, we demonstrate, for the first time, that XO has an unexpected protective role during hemolysis. Using an established hemolysis model, we found that intravascular hemin challenge (40 μmol/kg) resulted in a significant increase in hemolysis and an immense (20-fold) elevation in plasma XO activity in Townes sickle cell phenotype (SS) sickle mice compared to controls. Repeating the hemin challenge model in hepatocyte-specific XO knockout mice transplanted with SS bone marrow confirmed the liver as the source of enhanced circulating XO as these mice demonstrated 100% lethality compared to 40% survival in controls. In addition, studies in murine hepatocytes (AML12) revealed hemin mediates upregulation and release of XO to the medium in a toll like receptor 4 (TLR4)-dependent manner. Furthermore, we demonstrate that XO degrades oxyhemoglobin and releases free hemin and iron in a hydrogen peroxide-dependent manner. Additional biochemical studies revealed purified XO binds free hemin to diminish the potential for deleterious hemin-related redox reactions as well as prevents platelet aggregation. In the aggregate, data herein reveals that intravascular hemin challenge induces XO release by hepatocytes through hemin-TLR4 signaling, resulting in an immense elevation of circulating XO. This increased XO activity in the vascular compartment mediates protection from intravascular hemin crisis by binding and potentially degrading hemin at the apical surface of the endothelium where XO is known to be bound and sequestered by endothelial glycosaminoglycans (GAGs).

* Corresponding author. West Virginia University School of Medicine, Department of Physiology and Pharmacology, 3074 Health Sciences Center North, 1 Medical Center Dr., Morgantown, WV, 15902, USA.
** Corresponding author. University of Pittsburgh School of Medicine, Department of Pharmacology and Chemical Biology, Heart, Lung, Blood and Vascular Medicine Institute, E1254 Biomedical Science Tower, 200 Lothrop St., Pittsburgh, PA, 15216, USA.
E-mail addresses: eric.kelley@hsc.wvu.edu (E.E. Kelley), astraub@pitt.edu (A.C. Straub).
[1] Current address: Department of Pathology, University of Alabama at Birmingham. Birmingham, AL, USA.

https://doi.org/10.1016/j.redox.2023.102636
Received 18 January 2023; Received in revised form 9 February 2023; Accepted 11 February 2023
Available online 13 February 2023

1. Introduction

Hemolytic conditions are associated with a plethora of disease processes affecting millions of people worldwide each year. These diseases include but are not limited to sickle cell disease (SCD) (~300,000 new patients per year) [1], malaria (~214 million cases and 429,000 deaths per year) [2], sepsis (30 million cases resulting in 8 million deaths per year) [3,4], and complications related to cardiac bypass (one of the most common surgical procedures performed on 44 per 100,000 people annually) [5] and transplantation (~140,000 solid organ transplants in 2019) [6]. Hemolysis releases hemoglobin and hemin into the circulation saturating canonical scavenging mechanisms (hemopexin and haptoglobin, respectively) leading to an excess of circulating free hemin and hemoglobin [7]. Free hemin can directly generate oxidants resulting in endothelial dysfunction and indirectly by upregulating enzymatic sources of oxidants ultimately leading to overt endothelial and organ damage [7,8]. Hemin is also a known agonist of toll-like receptor 4 (TLR4), a receptor that can activate endothelial cells and macrophages to induce an inflammatory response [9].

SCD is caused by a single point mutation in the beta chain of hemoglobin that causes polymerization of hemoglobin protein resulting in the characteristic sickling of red blood cells (RBCs) [10,11]. Sickled RBCs become lodged in the microcirculation, resulting in vaso-occlusive episodes. Consequently, RBCs are also prone to hemolyze due to auto-oxidation of sickle oxyhemoglobin releasing free hemin locally in the circulation [12–14]. Free hemoglobin and hemin are two of the key drivers of pathology in SCD. The combination of cell free hemoglobin and increased oxidant production decreases nitric oxide (NO) bioavailability, a critical molecule for vascular homestasis [15]. Free hemin can act as a peroxidase to generate oxidants that mediate overt damage to endothelial cells as well as signal through TLR4 to activate endothelial cells and macrophages inducing a sterile inflammatory response [8]. In the Cooperative Study of Sickle Cell Disease, sickle patients actively experiencing a hemolytic episodic event demonstrated potential cell free hemoglobin and hemin concentrations 50–60 μM versus <5 μM for heathy individuals and thus are strong predictors of mortality [16]. Increases in free hemin deplete the scavenging molecule, hemopexin and accordingly, SCD patients have been reported to have hemopexin concentrations as low as 0.24 mg/mL [17-19], compared to 400–1500 mg/mL in healthy individuals [20]. The chronic hemolysis caused by SCD leaves patients unable to manage elevated hemin released during an episodic event. While there have been recent drug developments, there are currently no Food and Drug Administration approved therapeutics to directly attenuate hemolysis in SCD.

One enzyme reported to have elevated activity in the circulation of SCD patients and mouse models, as well as several other hemolytic conditions is xanthine oxidase (XO) [8,21–23]. XO is one form of the enzyme collectively known as xanthine oxidoreductase (XOR) with the other form being xanthine dehydrogenase (XDH) [8,24]. XOR is a key enzyme in the purine degradation pathway, oxidizing hypoxanthine to xanthine and xanthine to uric acid [21]. This pathway is critical in SCD and other hemolytic conditions as hemolysis releases ATP, and possibly one of the reasons XO levels are elevated in SCD [25]. XOR consists of three domains: a molybdenum cofactor, two non-identical iron-sulfur clusters, and an FAD [8]. XDH is converted to XO via stress-mediated post translational modifications that alter the structure adjacent to the FAD domain, the main structural difference between XDH and XO [8,20]. XDH utilizes NAD^+ as an electron acceptor; however, the conformational changes adjacent to the FAD in XO diminish affinity for NAD^+ and elevate affinity for oxygen [8,20]. As a result, XO produces hydrogen peroxide (H_2O_2) and superoxide ($O_2^{\bullet-}$) as a byproduct of hypoxanthine/xanthine oxidation [8]. XDH demonstrates its greatest specific activity in the liver; however, following hepatic stressors such as inflammation, ischemia, and hypoxia, XDH is postulated to be released to the circulation and rapidly converted into XO via plasma proteases [26]. The mechanism of hepatic XDH release, while assumed operative for decades, has never been characterized (*e.g.,* requisite signaling, mechanism of exocytosis, proof that circulating XO is derived from the liver). Once in circulation, XO can bind with high affinity ($K_d = 6$ nM) to distal vascular beds via electrostatic interactions with glycosaminoglycans (GAGs) to produce an endothelial micro-environment with a sequestered source of oxidant production [26]. For this reason, excess XO has almost exclusively been described as contributory to poor outcomes in pathological conditions. However, if this were indeed the case, then XOR might not have survived the evolutionary process in such a tightly conserved manner, affirming the potential existence of salutary functions that have yet to be identified. Addressing this issue specifically, we demonstrate that XO assumes a protective role during intravascular hemin crisis.

Abbreviations

XO	xanthine oxidase
ROS	reactive oxygen species
XDH	xanthine dehydrogenase
SCD	sickle cell disease
TLR4	toll like receptor 4
GAG	glycosaminoglycan
RBC	red blood cell
NO	nitric oxide
XOR	xanthine oxidoreductase
ACD	acid citrate dextrose
PRP	platelet rich plasma
PGI2	prostaglandin I2
RIPA	ristocetin induced platelet activation
DETA NONOate	(Z)-1-[2-(2- Aminoethyl)-N-(2-ammonioethyl) amino]diazen-1-ium-1,2-diolate
MCV	mean corpuscular volume
RDW	red cell distribution width
MPV	mean platelet volume
AML12	alpha mouse liver 12
AUC	area under the curve
EPR	electron paramagnetic resonance
HS	heparan sulfate
CS	chondroitin sulfate

2. Materials and methods

2.1. Animals

Eight-week-old C57BL/6J (23 wildtype; stock no. 000664) mice were ordered from the Jackson Laboratory (Bar Harbor, ME). $Xdh^{floxed/floxed}Alb\text{-}1^{Cre/Wt}$ (Albumin-1; 6 hepatocyte-specific Xdh knockout) [27], $Xdh^{floxed/floxed}Alb\text{-}1^{Wt/Wt}$ (5 littermate floxed [FLX] controls) [27], and sickle (SS) and control (AA) Townes knock-in mice were bred and maintained at the University of Pittsburgh. The $Xdh^{floxed/floxed}$ mice were bred on a C57BL/6J background and the SS and AA Townes mice were bred on a combination of a C57BL/6J and 129S background [28]. Seven-to fourteen-week-old male mice were used for experiments. Female mice were not included in this study because there is currently no

evidence of sex differences in SCD-related hemolysis. In Townes mice, the murine alpha and beta genes are knocked out and replaced with human hemoglobin genes [29]. The AA control mice contain two human alpha and beta hemoglobin transgenes, while the SS sickle mice contain two alpha and two mutant sickle beta hemoglobin transgenes [29]. All animal experiments were reviewed and approved by the Institutional Animal Care and Use Committee at the University of Pittsburgh. The mice were all supplied a normal chow diet (no. 5234), had free access to drinking water, and were housed in pathogen free conditions in accordance with the Guide for the Care and Use of Laboratory Animals from the Department of Laboratory Animal Research at the University of Pittsburgh.

2.2. Bone marrow transplanted chimeric mice

Genotyping of the $Xdh^{floxed/floxed}$ mice was performed using polymerase chain reaction analysis of DNA isolated from tail tissue. Peripheral hemoglobin electrophoresis was used to genotype the AA and SS Townes mice using Hb (E) and Hb (E) Acid kits (Sebia Capillary System; Lisse, France), according to the guidelines provided by the manufacturer. The blood was spun down at 2,500×*g* for 10 min and the plasma was removed. Five μL of the RBC pellet was combined with 65 μL of Sebia hemolysis solution, vortexed, and incubated at room temperature for 10 min. Samples were then incubated in a humidity chamber for 5 min before running on an agarose gel and staining of hemoglobin bands. The C57BL/6J-AA mice received bone marrow from AA Townes mice and the C57BL/6J-SS, $Xdh^{floxed/floxed}Alb\text{-}1^{Cre/Wt}$/SS, and $Xdh^{floxed/floxed}Alb\text{-}1^{Wt/Wt}$/SS groups received bone marrow from SS Townes mice. The bone marrow transplants were performed as previously described [30]. Briefly, bone marrow cells were collected from the femurs and tibias of AA and SS Townes donor mice. C57BL/6J (8 weeks old), $Xdh^{floxed/floxed}Alb\text{-}1^{Cre/Wt}$ (7–14 weeks old), and $Xdh^{floxed/floxed}Alb\text{-}1^{Wt/Wt}$ (7–14 weeks old) recipient mice were lethally irradiated (two 500–550 rad doses, 3 h apart) before retro-orbital injection of isolated AA or SS Townes bone marrow cells (1.5–2.5 × 10^6 cells). After irradiation the mice were placed in fresh autoclaved cages and provided autoclaved chow and 0.2% neomycin drinking water for two weeks before returning to normal autoclaved drinking water. The mice were allowed 12 weeks to fully engraft, at which point 50–100 μL of blood was collected retro-orbitally to assess engraftment efficiency. Mice were anesthetized with 1% isoflurane and blood was collected using heparin coated microcapillary tubes. The whole blood was spun down at 2,500×*g* for 10 min to separate the RBC pellet and the plasma. Engraftment of the AA and SS Townes bone marrow was evaluated using the Sebia hemoglobin electrophoresis kit described above using the RBC pellet. The percentage of mouse wildtype versus AA or SS bone marrow was quantified using Phoresis software. Any mouse with <85–90% of the donor hemoglobin was excluded from the experiment. The mice were rested for two weeks before hemin challenge.

2.3. Hemin challenge and hematologic phenotyping

Hemin challenge was performed by injecting 40 μmol/kg of hemin (Frontier Scientific, H651-9) via tail vein into each mouse (200 μL). Hemin was made fresh for each experiment in 0.25 N NaOH (Fisher Chemical, S318-500) and brought to a pH of 7.4 using HCl. The mice were observed over a 24-h period at which point the surviving mice were euthanized for blood and tissue collection. Blood (300–600 μL) was collected via the vena cava in 5% 0.5 M, pH 8.0 EDTA (Promega, V4231). Complete blood counts were measured using a Heska (HemaTrue Inc.; Miami Lakes, FL) in accordance with the manufacturer's instructions. Reticulocytes were measured from whole blood using flow cytometry as described previously [31]. Briefly, Thiazole orange (80 pM in 1 × PBS; Santa Cruz, sc-215,967) was used to stain reticulocytes overnight at 4 °C and protected from light. Reticulocyte percentage was analyzed using flow cytometry (LSR-Fortessa; Becton Dickinson), and FACSDIVA software was used for data collection. Blood was spun down at 2,500×*g* for 10 min to separate the plasma and RBC pellet. Plasma was aliquoted and stored at −80 °C until further experiments. Mice were then perfused with 5 mL of 1xPBS, and organs were collected and snap-frozen in liquid nitrogen.

2.4. AML12 cell culture conditions and treatment

AML12 hepatocytes were grown in DMEM/F12 (ThermoFisher Scientific, Waltham, MA) media supplemented with dexamethasone, (ThermoFisher Scientific, Waltham, MA) growth supplement (ThermoFisher Scientific, Waltham, MA), and 10% FBS (ThermoFisher Scientific, Waltham, MA). For experiments, cells were seeded in 6-well plates. For genetic knockdown, cells at 70% confluency were transfected with 10 nM scrambled or TLR4 targeted siRNA (silencer select, ThermoFisher Scientific, Waltham, MA) using Lipofectamine 3000 (ThermoFisher Scientific, Waltham, MA). After cells reached 90% confluency, cells were washed with sterile PBS, then treated with 1 mL of MEM alpha supplemented with 16 μM hypoxanthine along with indicated treatments (10 μM hemin, 2.5 μM oxyhemoglobin, 10 μM TAK-242). Cells were cultured in MEM alpha for the indicated periods of time and the media was collected and snap frozen to analyze XO activity while the cells were collected in PBS with HALT phosphatase and protease inhibitors (ThermoFisher Scientific, Waltham, MA) or Qiagen RLT buffer for RNA extraction.

2.5. XO activity

Plasma and tissue (liver, lung, and kidney) XO activity were assessed as previously described [27,31]. Briefly, blood was collected at baseline via the retro-orbital vein and at the end point via the vena cava and plasma was isolated as described above. Tissue was snap frozen in liquid nitrogen. For cell culture experiments, media was collected from cells. XO activity was measured from all sources with electrochemical detection (Dionex UltiMate 3000 RS Electrochemical Detector) of uric acid post reverse-phase high-performance liquid chromatography separation.

2.6. XOR protein analysis

Samples were prepared with Laemmli sample buffer and β-mercaptoethanol and run on a 4–20% gradient gel (Biorad, Hercules, California) at 70 V. Samples were then transferred to 0.45 μm nitrocellulose membranes, dried, and reconstituted with ddiH_2O. Membranes were blocked with Li-Cor (Lincoln, Nebraska) TBS blocking buffer, and incubated in primary antibody overnight at 4 °C. Primary antibodies include β-actin (Santa Cruz Biotechnology, Dallas, Texas) and xanthine oxidoreductase (Santa Cruz Biotechnology, Dallas, Texas). Membranes were then washed with TBS containing 1% tween (TBST), incubated in Li-Cor near-infrared secondary antibodies for 1 h at room temperature, washed again with TBST, and finally imaged with the Li-Cor Odyssey Clx. Densitometry analysis was conducted in Image-J (National Institutes of Health, Bethesda, Maryland) and reported as target normalized to β-actin and fold change calculated from control.

2.7. XOR RNA analysis

RNA was extracted from AML12 cells by Qiagen RNeasy Kit per manufacturer's instructions. Following RNA extraction, RNA concentration was analyzed by nano-drop spectrophotometer and 1 μg of RNA was used in High-Capacity RNA-to-cDNA kit (Applied Biosystems ThermoFisher Scientific, Waltham, MA). Real-time PCR was then performed using iTaq SYBRgreen Supermix (Biorad, Hercules, California) on an Applied Biosystem Real-time PCR instrument. Primers: mouse XDH (IDT, forward: CCGCCTTCAGAACAAGATCG, reverse: CCTTCCACAGTTGTCACAGC) and mouse GAPDH (Takara). Data shown as fold

change from control.

2.8. Molecular modeling of XO and hemin

Molecular modeling was done using the Molecular Operating Environment (MOE 2020.09) from the Chemical Computing Group. The crystallographic structure of XO was obtained from the Protein Data Bank and downloaded as a PDB file: 1V97. In MOE, the structure was prepared for analysis by adding missing hydrogens and optimizing the structure to remove any steric classes. The pH was set at 7.4.

2.9. Hemin binding dot blot

Hemin binding was assessed by incubating mixtures of hemin (25 μM, Frontier Scientific, H651-9), xanthine oxidase purified from fresh cow's cream in the Kelley lab (50 μM) and hypoxanthine (100 μM; Sigma, H9377-5G) in the presence or absence of febuxostat (50 μM; Axon, TEI 6720) in PBS at room temperature for 20 min. An additional control in which albumin (50 μM) was incubated with hemin was included. Aliquots obtained at different timepoints were diluted in non-reducing Laemmeli buffer to stop the reaction and hemin binding was assessed by dot-blotting in nitrocellulose. The membrane is washed to remove free hemin and hemin bound to XO is assessed by chemiluminescent detection with Clarity Western ECL reagent (Bio-Rad). The presence of bound hemin is detected by the peroxide reagent in the Clarity Western ECL reacting with the hemin (to produce compound I) as it would with traditional HRP-conjugates to further react with luminol and produce light. Images were acquired using a ChemiDoc XRS + imaging station and dot density was quantified with the included ImageLab Software 5.2.1 (Bio-Rad).

2.10. Platelet activation

Whole blood was collected from healthy human volunteers, according to University of Pittsburgh Institutional Review Board–approved protocols, in acid-citrate dextrose (ACD) solution-A anticoagulant and platelet rich plasma (PRP) was separated by centrifugation at 500×*g*, for 20 min at 25 °C in swinging buckets. Prostaglandin I2 (PGI2; 1 μg/mL) was added to the PRP, and platelets were pelleted down by centrifugation at 1500×*g*, 25 °C for 10 min. The platelets were washed with erythrocyte lysis buffer containing PGI2 to remove residual red cells (centrifuged at 1500×*g*, 25 °C for 5 min) and resuspended in modified Tyrode's buffer (20 mM HEPES, 128 mM NaCl, 12 mM sodium bicarbonate, 0.4 mM sodium phosphate monobasic, 5 mM dextrose, 1 mM $MgCl_2$, 2.8 mM KCl, pH 7.4). The platelet count was determined by Hemavet® 950. The platelet count was adjusted to 2.0–2.5 × 10 [6]cells/mL with modified Tyrode's buffer for all treatments. The platelets were pretreated with purified XO (10 mU/mL), and hypoxanthine (200 μM; Sigma, H9377-5G) or purified XO (10 mU/mL), hypoxanthine (200 μM; Sigma, H9377-5G) and febuxostat (20 μM; Axon, TEI 6720) for 30 min at room temperature, followed by hemin (2.5 μM; Frontier Scientific, H651-9) treatment for 20 min. Treated platelets were stained with anti-CD41a-PE (BD Pharmingen, 555,467) and anti-CD62P (P-selectin)-APC (BD Pharmingen, 550,888) and the platelet activation was measured using flow cytometry (LSR-Fortessa; Becton Dickinson) by estimating the surface level of P-selectin on the CD41a positive population. Data was analyzed using FlowJo™ v10.8.1 software.

2.11. Platelet aggregation

PRP was separated from whole blood collected from healthy human volunteers, according to University of Pittsburgh Institutional Review Board–approved protocols, in sodium citrate (3.2%) anticoagulant by centrifuging at 500×*g*, 25 °C in swinging buckets. The collected PRP was treated with the combinations of febuxostat (20 μM; Axon, TEI 6720), purified XO (10 mU/mL), and hypoxanthine (200 μM; Sigma, H9377-5G) for 30 min, followed by hemin (2.5 μM; Frontier Scientific, H651-) treatment for 20 min at room temperature. The treated PRP was subjected to ristocetin (0.5 mg/mL)-induced platelet aggregation (RIPA) (Bio/Data™ 100,970) using CHRONO-LOG® Model 700 Optical Aggregometer. The data was analyzed using AGGRO/LINK®8.

2.12. Generation of oxyhemoglobin

Human hemoglobin (Sigma Aldrich, H7379) was dissolved in PBS (20 mg/mL) and mixed gently. The hemoglobin was spun down at 7,000×*g* for 5 min and the supernatant was isolated. Dithionite (50 mM; Sigma) was added to the hemoglobin and passed through the column in 500 μL aliquots. The dithionite was removed by size exclusion chromatography (G25 Sephadex PD10 column, GE analytics, U.S.). The PD10 column was prepared by rinsing with 50 mL of water, followed by 50 mL of PBS.

2.13. XO/OxyHb UV-VIS spectroscopy

Oxyhemoglobin (17 μM; Sigma Aldrich, H7379) was incubated with combinations of purified XO (50 mU/mL), xanthine (400 μM; Sigma), and catalase (10 U/mL; Calbiochem) in PBS for 20 min. Absorbance was measured with a spectrophotometer (UV-VIS recording spectrophotometer UV-2401 PC, Shimadzu Scientific Instruments) every 2 min for 20 min following initiation of the reaction.

2.14. Electron paramagnetic resonance (EPR) spectrometry

Combinations of sodium ascorbate (1 mM; Sigma-Aldrich, #255564), oxyhemoglobin (17 μM; Sigma Aldrich, H7379), purified XO (50 mU/mL), xanthine (400 μM; Sigma), catalase (1 kU/mL; Calbiochem), and diethylenetriaminepentaacetic acid (DTPA; 50 μM; Sigma) were mixed in PBS (pH 7.4) for EPR detection. Reactions were incubated for 15 min at 37 °C then the ascorbate was added and incubated for another 5 min again at 37 °C. After incubation, the samples were snap frozen in liquid nitrogen and stored at −80 °C until EPR experiments/analysis were carried out. Ascorbate ($AscH_2$) (EPR silent) is oxidized by reactive/Fe(III) species to form the ascorbate radical ($Asc^{\bullet-}$) (EPR active). EPR spectroscopy was used to measure the formation of ascorbate radical [32] At the time of EPR measurements, frozen samples were rapidly thawed and loaded (50 μL) into a glass capillary tube (Ref: 9600150; Hirschmann Laborgerate GmbH & Co. KG, D-74246 Eberstadt, Germany). The sample loaded capillary tubes were sealed on one end using Critoseal clay and placed inside the 4 mm (O.D) EPR quartz tube (Catalog: 707-SQ-250 M; Wilmad LabGlass, Vineland, NJ, USA). The quartz tube was positioned inside the cavity/resonator and EPR spectra were recorded at room temperature. EPR spectra were recorded using a Bruker EMXnano spectrometer (Bruker BioSciences, Billerica, MA, USA) operating at X-band with a 100 kHz modulation frequency as described previously [32,33]. The following EPR instrument parameters were used: microwave frequency, 9.617 GHz; center field, 3425 G; sweep width, 20 G; microwave power, 20 mW; modulation amplitude, 0.5 G; modulation frequency, 100 kHz; receiver gain, 60 dB; time constant, 5.12 ms; conversion time, 37.5 ms; sweep time, 30 s; number of scans, 10. Data acquisition was performed using Bruker Xenon_nano software. The signal intensity was measured using first peak (low field) height of the EPR spectrum and normalized to the background signal of OxyHb + Asc. Data processing was performed using GraphPad Prism 9 (GraphPad software, San Diego, CA).

2.15. Nitric oxide (NO) consumption assay

Oxyhemoglobin (17 μM; Sigma Aldrich, H7379) was incubated with combinations of purified XO (5 μM; obtained from Kelley lab), and xanthine (400 μM; Sigma), and NO consumption was measured as

previously described [34]. Briefly, 40 μM of the NO donor (Z)-1-[2-(2-Aminoethyl)-N-(2-ammonioethyl)amino]diazen-1-ium-1, 2-diolate (DETA NONOate; Cayman) in PBS (pH 7.4) was added to a glass container with a continuous flow of helium. Once the NO signal stabilized at ~20 mV, the reaction mixtures were added to the glass container. Measurements of the decrease in NO with each reaction were recorded using a Sievers Nitric Oxide Analyzer (General Electric) and quantified using ImageJ by calculating the area under the curve as a measure of NO consumption.

2.16. Statistics

ROUT analysis with a Q = 1% was used to identify outliers and if identified they were excluded from the dataset. When comparing two groups, a Shapiro-Wilk test was used to assess the normality of the data. If the data was normally distributed an unpaired Student *t*-test was used to compare the groups. If the standard deviation of the groups was significantly different a Welch's correction was added. If the data was not normally distributed the two groups were compared using a Mann-Whitney test. When three or more groups were compared a 1-way ANOVA with Dunnett multiple comparison test was used when comparing multiple groups to a control group or Sidak multiple comparison test if multiple comparisons were made. Significance for all statistical tests were defined as $P < 0.05$.

3. Results

3.1. XO is released into circulation in response to hemin crisis

To investigate the effects of hemolysis on circulating XO activity we transplanted AA control or SS sickle Townes bone marrow into 8-week-old C57BL/6J mice (Fig. 1A). The mice were allowed 12-weeks to fully engraft at which point the WT SS mice developed SCD and mice less than 90% AA or SS engraftment were excluded (Supplemental Fig. 1A). Blood was collected at baseline and 14 days later the mice were challenged with 40 μmol/kg hemin via tail vein injection, a dose similar to previous publications [35]. The mice were euthanized 24 h later for blood and tissue collection. The WT AA mice had 100% survival over the 24-h period; however, only 75% (9/12) of the WT SS mice survived (Supplemental Fig. 1B). Complete blood counts were used to assess the degree of hemolysis as a delta change from baseline to 24 h post-hemin challenge. The WT AA and WT SS mice both had some degree of hemolysis as demonstrated by a decrease in RBCs, hematocrit, and hemoglobin; however, the WT SS mice had a significantly greater loss in hematocrit ($P < 0.0001$) and hemoglobin ($P = 0.0018$) compared to the WT AA mice (Fig. 1B–D). A complete list of hematological parameters is included in Supplemental Table I. There was a significant decrease in mean corpuscular volume (MCV) and reticulocytes, and a significant increase in red cell distribution width (RDW) and mean platelet volume (MPV) in the WT SS mice compared to the WT AA mice (Supplemental Table I). This could suggest that hemin challenge in WT SS mice has greater effect on RBC and platelet size which could be the result of formation of more RBC-platelet aggregates compared to the WT AA mice. Next, we assessed the extent of XO release into circulation by measuring plasma XO activity as a delta change from baseline to 24 h post-hemin injection. While the WT AA mice had a modest 58.67 μU/mL increase in plasma XO activity, the WT SS demonstrated a 20-fold (1216 μU/mL) greater increase in plasma XO activity, with similar trends in the plasma uric acid concentration (Fig. 1E and Supplemental Table II). These data suggest that WT SS mice were more susceptible to the hemin challenge, resulting in a greater increase in plasma XO activity.

3.2. The liver (hepatocytes) is likely the source of XO elevated in hemin crisis

To assess the anatomic/cellular source of XO contributing to elevation in circulating XO levels during hemin challenge we used a hepatocyte-specific XDH knockout mouse. SS sickle Townes bone marrow was transplanted into 7–14-week-old $Xdh^{floxed/floxed}Alb\text{-}1^{Cre/Wt}$ ($HXdh^{-/-}$) or $Xdh^{floxed/floxed}Alb\text{-}1^{Wt/Wt}$ ($HXdh^{fl/fl}$) mice and allowed 12

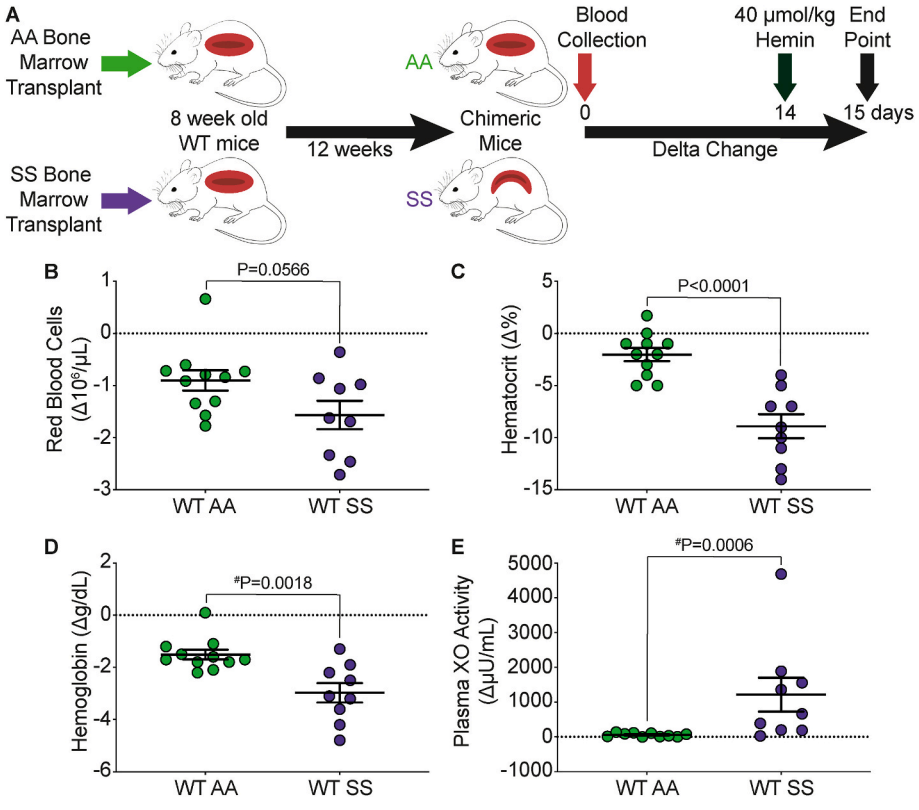

Fig. 1. WT SS mice have a significant increase in plasma XO activity in response to hemin crisis. A) Experimental design. Complete blood counts shown as a delta change from baseline to 24 h post-hemin challenge including **B)** red blood cells, **C)** hematocrit, and **D)** hemoglobin. **E)** Plasma XO activity was measured using HPLC as a delta change from baseline to 24 h post-hemin challenge. Values are mean ± SEM using an unpaired Student *t*-test unless otherwise noted. #Values are mean ± SEM using a Mann Whitney test. WT, wildtype; XO, xanthine oxidase; HPLC, high performance liquid chromatography. (For interpretation of the references to color in this figure legend, the reader is referred to the Web version of this article.)

weeks to fully engraft (Fig. 2A). Bone marrow engraftment was assessed after 12 weeks using hemoglobin gel electrophoresis and 85% was used as a cutoff for inclusion in the experiment (Supplemental Fig. 2). Blood was collected for baseline measurements and 14 days later the mice were challenged with 40 μmol/kg hemin. The mice were observed for 24 h following hemin injection and tissue was collected (Fig. 2A). All the HXdh$^{-/-}$ mice (n = 6) died between 4 and 20 h post-hemin injection; however, 40% of the HXdh$^{fl/fl}$ mice (n = 5) survived for 24 h post-hemin injection (Fig. 2B). To evaluate the efficacy of the mouse model we measured liver, lung, and kidney XO activity following hemin challenge. As expected, the HXdh$^{-/-}$ mice demonstrated a significant reduction in liver XO activity with no impact on lung or kidney XO activity (Fig. 2C, Supplemental Table III). Unfortunately, the majority (5/6) of the HXdh$^{-/-}$ mice died before we could collect blood and thus validate diminished circulating XO levels in response to hemin challenge compared to controls.

3.3. Hepatocyte XO release occurs through hemin-TLR4 signaling

To more clearly understand how hemin challenge results in such a large increase in circulating XO activity we used alpha mouse liver 12 (AML12) cells to determine the mechanism of XO release to the media. AML12 cells were treated with 10 μM hemin and media was collected for XO activity assessment between 0 and 16 h after hemin treatment. Media XO activity began to increase within the first 5 min after hemin treatment, with continued elevation of XO in the media at 8 and 16 h (Fig. 3A).

Hemin is a known agonist for TLR4 [9], and we hypothesized that hemin-TLR4 signaling was involved in the mechanism for hepatic XO release. To test this hypothesis, TLR4 was knocked down using siRNA in AML12 cells for 48 h (knockdown efficiency = 62%; Supplemental Fig. 3A) followed by treatment with 10 μM hemin. Knockdown of TLR4 resulted in complete inhibition of hemin-mediated XO release in AML12 cells 24 h after treatment (Fig. 3B). Additionally, pharmacologic inhibition of TLR4 with the inhibitor TAK242 for 30 min prior to treatment with 10 μM hemin also resulted in complete inhibition of hemin-mediated hepatic XO release 24 h after treatment (Fig. 3C). The specificity of hemin-TLR4 mediated hepatic XO release was evaluated by treating AML12 cells with 2.5 μM oxyhemoglobin and measuring XO activity from the media of the cells. Oxyhemoglobin did not result in an increase in XO release from AML12 cells and pre-incubation with TAK242 for 30 min prior to oxyhemoglobin treatment had no effect on media XO activity (Fig. 3D). To test if XO was merely released from hepatocytes or expression was upregulated, XO RNA and protein levels were measured from AML12 cells treated with TAK242 for 30 min prior to treatment with 10 μM hemin. Hemin treatment resulted in a 2.8-fold increase in XOR mRNA; however, pre-treatment with TAK242 prevented the increase in mRNA expression (Fig. 3E). Similarly, hemin treatment resulted in a 2.2-fold increase in XOR protein expression that was reduced to a 1.4-fold increase in XOR when pre-treated with TAK242 (Fig. 3F and Supplemental Fig. 3B), suggesting that hemin-TLR4 signaling releases XO from hepatocytes and upregulates XOR expression.

3.4. XO-derived H_2O_2 facilitates hemoglobin degradation and its capacity to bind NO

In addition to hemin, hemolysis releases hemoglobin which can exert deleterious vascular consequences, including NO sequestration, if it is not scavenged and degraded. To investigate the effects of XO activity on hemoglobin, we incubated 17 μM oxyhemoglobin with 50 mU/mL XO and 400 μM xanthine for 20 min and observed a visible color change in the reaction mixture compared to the oxyhemoglobin alone (Fig. 4A, **left and middle**). When 1 kU/mL of catalase was added to the reaction mixture there was no visible color change in the oxyhemoglobin, suggesting oxyhemoglobin degradation is H_2O_2-dependent (Fig. 4A, right). Oxyhemoglobin (17 μM) was incubated with XO (50 mU/mL) and xanthine (400 μM) for 20 min and the absorbance was measured every 2 min. There was a time-dependent decrease in absorbance at the 415 nm peak (Soret band), as well as at the doublet peaks between 500 and 600 nm, consistent with the color change observed by eye and suggestive of hemoglobin degradation (Fig. 4B). Closer examination of the doublet peaks between 500 and 600 nm reveals the formation of two isosbestic points at ~525 and ~580 nm (Fig. 4C). This suggests there is oxyhemoglobin degradation and formation of additional species.

To further validate XO-mediated hemoglobin degradation and release of hemin and or Fe, we measured ascorbate radical production using electron paramagnetic resonance (EPR). The rationale here was that degradation of hemoglobin would lead to release of hemin and iron that would readily oxidize ascorbate (hemin-Fe^{3+} or Fe^{3+} + $AscH^-$ → hemin-Fe^{2+} Fe^{2+} + $Asc^{\bullet}$). Samples were incubated for 20 min prior to EPR measurement. Ascorbate alone produced a small amount of ascorbate radical as observed by the doublet near $g = 2$; however, addition of oxyhemoglobin to ascorbate did not significantly elevate this background ascorbate radical signal indicating that the 4 iron-containing porphyrins (hemin) are not redox active and that contamination of the preparation with Fe or hemin was minimal. This allowed us to normalize values to the ascorbate + oxyhemoglobin signal intensity (Fig. 4D–E). However, incubation of ascorbate and oxyhemoglobin + XO and

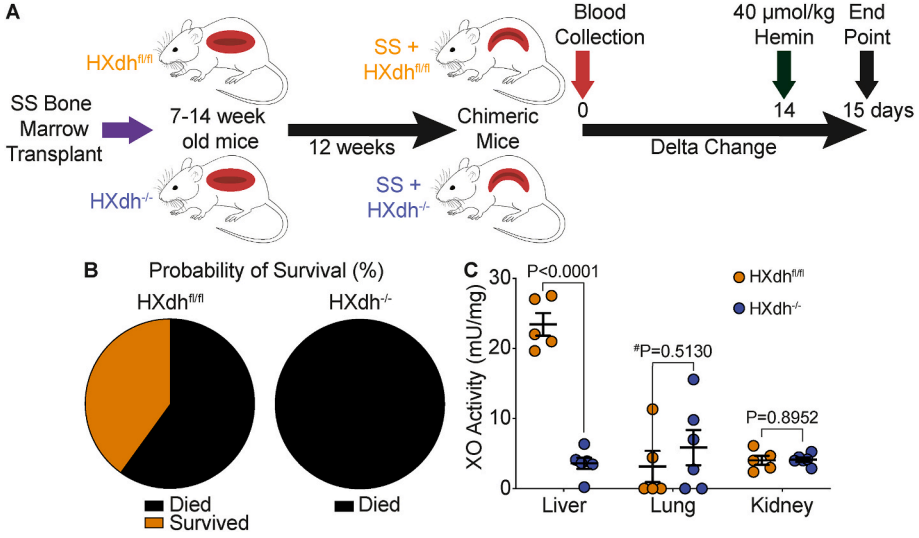

Fig. 2. Hepatocyte specific XO knockout decreases survival following hemin challenge. A) Experimental design. **B)** Survival was measured over the 24 h following hemin challenge in HXdh$^{fl/fl}$ (n = 5) and HXdh$^{-/-}$ mice (n = 6). The HXdh$^{fl/fl}$ mice had a 40% survival rate, while all the HXdh$^{-/-}$ mice died within 20 h. **C)** Liver, lung, and kidney tissue was collected at time of death or 24 h post-hemin injection and XO activity was measured using HPLC. Values are mean ± SEM using an unpaired Student *t*-test unless otherwise noted. #Values are mean ± SEM using a Mann Whitney test. Xdh, xanthine dehydrogenase; XO, xanthine oxidase; HPLC, high performance liquid chromatography.

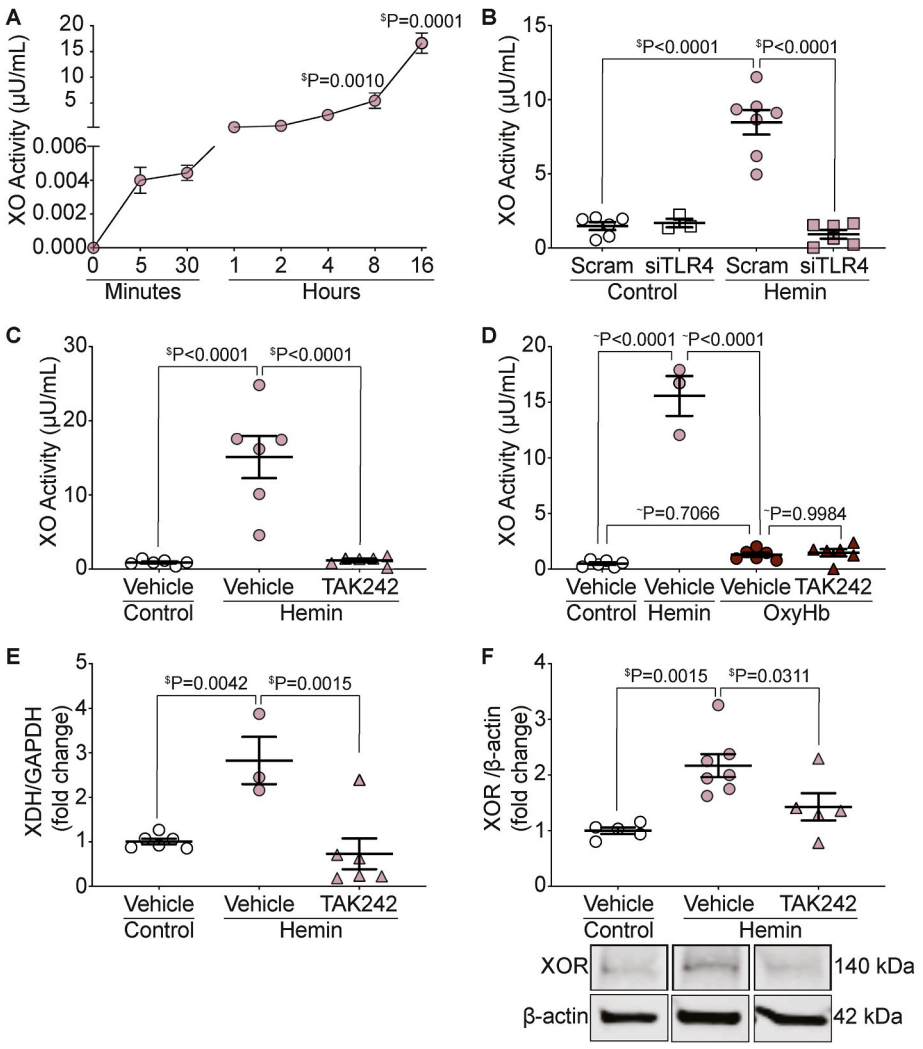

Fig. 3. Hemin-TLR4 signaling releases XO from AML12 cells. A) AML12 cells were treated with 10 μM hemin and media was collected between 0 min and 16 h after treatment for XO activity measurement using HPLC. **B)** AML12 cells were treated with scrambled or siTLR4 for 48 h prior to treatment with 10 μM hemin. Media was collected and XO activity was measured. **C)** AML12 cells were treated with the TLR4 inhibitor TAK242 for 30 min prior to treatment with 10 μM hemin. Media was collected and XO activity was measured. **D)** AML12 cells were treated with TAK242 for 30 min prior to treatment with 10 μM hemin or 2.5 μM oxyhemoglobin. Media was collected and measured for XO activity. AML12 cells were treated with TAK242 for 30 min prior to treatment with 10 μM hemin. Cellular XOR mRNA **E)** and protein **F)** were measured from the cells by qPCR and Western blot. $Values are mean ± SEM using a 1-way ANOVA with Dunnett multiple comparisons test. ¯Values are mean ± SEM using a 1-way ANOVA with Sidak's multiple comparisons test. XO, xanthine oxidase; AML, alpha murine liver; Scram, scrambled; TLR4, toll like receptor 4; OxyHb, oxyhemoglobin; XOR, xanthine oxidoreductase; HPLC, high performance liquid chromatography.

oxyhemoglobin + xanthine + XO modestly or greatly increased ascorbate radical formation, respectively, which can be attributed to hemin-Fe^{3+} and free ferric iron being released from oxyhemoglobin and reacting with ascorbate (Fig. 4D–E). Next, we added catalase or DTPA to the reaction mixture and observed a significant reduction in the production of ascorbate radical (Fig. 4D–E) suggesting the breakdown of oxyhemoglobin and formation of ascorbate radicals is dependent on H_2O_2 production and iron release.

NO binds specifically to the ferrous form (Fe^{2+}) of hemoglobin, known as oxyhemoglobin ($K_D = 10^{-10}$-10^{-11} M) to form methemoglobin and nitrate [36]. This deoxygenation reaction scavenges NO and inhibits NO-mediated signaling [36]. Therefore, we hypothesized that if XO activity mediates degradation of a hemoglobin preparation then this preparation should demonstrate diminished capacity to scavenge NO. To test this hypothesis, we performed an NO consumption assay. The addition of oxyhemoglobin an equilibrated NO donor-mediated production and resultant flow of NO in the nitric oxide analyzer (NOA) results in a drop in voltage, indicating oxyhemoglobin scavenges NO as expected (Fig. 4F). When oxyhemoglobin is incubated with XO for 20 min prior to addition, there is a small, but insignificant decrease in the area under the curve; however, when xanthine was added to the reaction mixture to provide substrate for XO activity, the area under the curve was significantly reduced (Fig. 4F–G). This suggests that XO activity prevents oxyhemoglobin from scavenging NO and provides further evidence of a protective mechanism for XO during hemin crisis.

3.5. XO binds hemin and protects against platelet activation and aggregation

While XO-derived peroxide can mediate hemoglobin degradation, to fully understand XO's contributions to protection from intravascular hemolysis one must account for elevated abundance of free hemin. As such, computational modeling of XO and hemin identified a predicted hemin binding site (K_D = 128 nM) within the FAD domain of XO (Fig. 5A). To assess the possibility of hemin-XO interaction, a hemin binding dot blot was performed by incubating hemin with XO for 20 min and the reactions were stopped using Laemelli buffer. Hemin binding was assessed by dot-blotting in nitrocellulose followed by chemiluminescent detection utilizing bound hemin as a horse radish peroxidase (HRP) mimic. Hemin alone was used to normalize the other conditions and account for nonspecific binding to the membrane. Incubation of hemin and XO resulted in a 2-fold increase in signal, indicating a hemin-XO interaction (Fig. 5B). When hemin was incubated with XO and hypoxanthine, there was a four-fold increase in signal, suggesting the enzymatic turnover of XO could play a role in the ability/extent of XO to bind hemin (Fig. 5B). Addition of febuxostat to the reaction mixture completely blunted the increase in dot density, confirming an activity (enzyme turnover)-dependent interaction of hemin and XO (Fig. 5B). However, for the XO-hemin binding to be significant *in vivo*, one must account for alternative hemin binding partners. For example, albumin accounts for 55–60% of all plasma proteins and can bind a wide range of ligands in the blood including hemin (K_D = 40 μM) [37,38]. To confirm

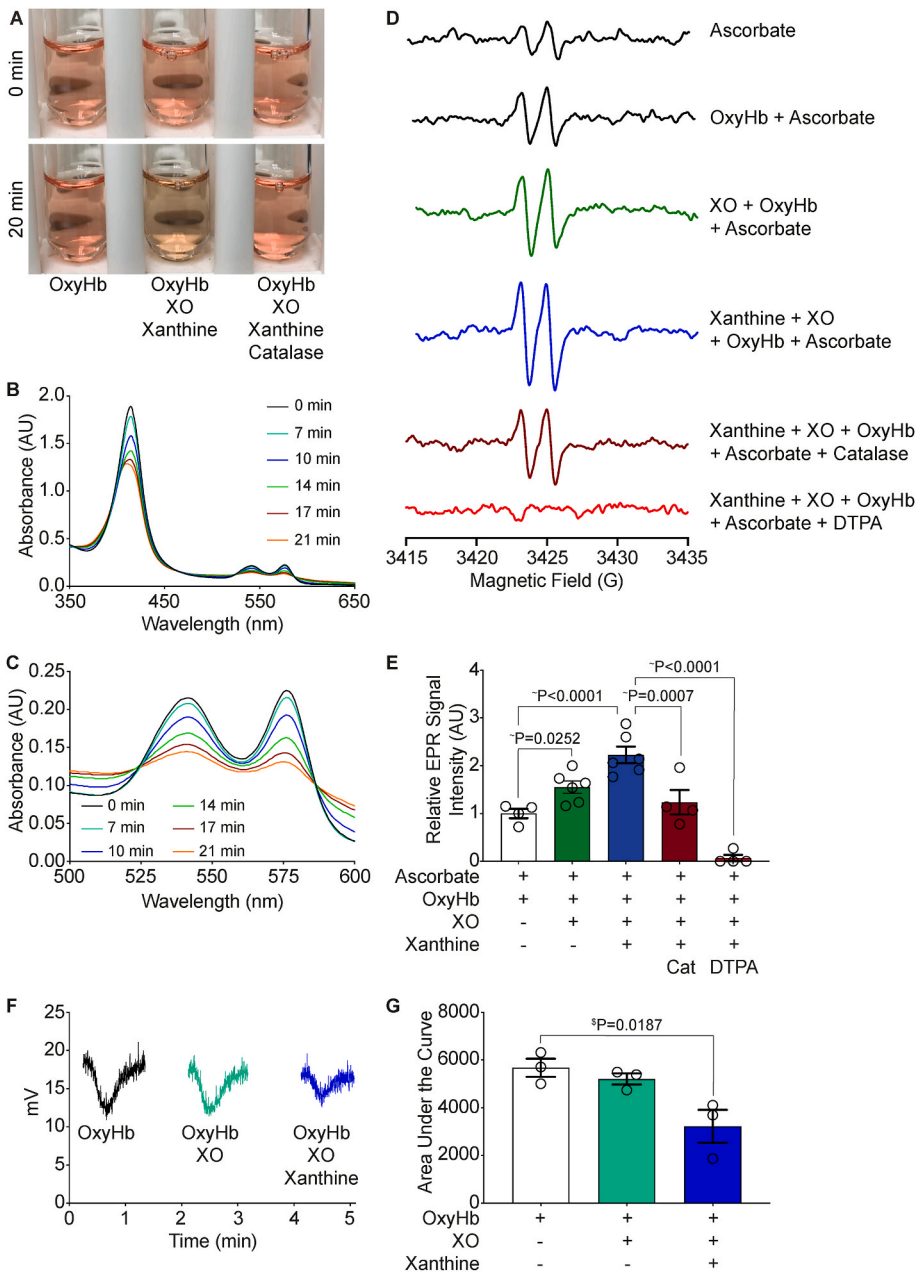

Fig. 4. XO activity facilitates oxyhemoglobin degradation. Oxyhemoglobin (17 μM) was incubated with XO (50 mU/mL) and xanthine (400 μM) for 20 min. Degradation of oxyhemoglobin and loss of iron was evaluated by eye **A)** and spectrophotometer **B–C). D)** EPR was used to follow the production of the ascorbate radical for assessing free iron and oxidant production. Oxyhemoglobin (17 μM) was incubated with ascorbate for 20 min prior to EPR measurement. **E)** Oxyhemoglobin (17 μM) was incubated with combinations of XO (50 mU/mL), and xanthine (400 μM) for 20 min and the relative signal intensity was normalized to ascorbate and oxyhemoglobin alone. **F)** DETA NONOate was used to create a continuous flow of 40 μM NO. Each reaction was added to the Sievers Nitric Oxide Analyzer sparger and NO consumption was quantified as **G)** area under the curve. $^{\$}$Values are mean ± SEM using a 1-way ANOVA with Dunnett multiple comparisons test. ¯Values are mean ± SEM using a 1-way ANOVA with Sidak's multiple comparisons test. Min, minute; OxyHb, oxyhemoglobin; XO, xanthine oxidase; DTPA, Diethylenetriamine pentaacetate; EPR, electron paramagnetic resonance; DETA NONOate, (Z)-1-[2-(2-Aminoethyl)-N-(2-ammonioethyl)amino]diazen-1-ium-1,2-diolate; NO, nitric oxide.

the specificity of XO-hemin interaction, albumin was incubated with hemin for 20 min and then assessed via dot blot as above. The albumin-exposed hemin samples demonstrated a 3-fold increase in signal, which was less than the 4-fold increase in signal with hemin, XO, and hypoxanthine (Supplemental Fig. 4A).

Scavenging of hemin by XO could provide some mechanism of protection during hemin challenge so we investigated the ability of XO to mediate hemin-induced platelet activation and aggregation. Platelets were isolated from healthy human blood and incubated with combinations of XO, hypoxanthine, and febuxostat for 30 min prior to activation with hemin. Flow cytometry was used as a measurement of platelet activation, while aggregation was measured using an aggregometer (Fig. 5C). Platelet activation was evaluated by staining for the platelet marker CD41a and the platelet activation marker CD62p. The non-treated platelets had a minimal amount of platelet activation (10%), while 94% of the platelets were activated by the positive control thrombin and 72% of platelets were activated by hemin alone (Fig. 5D–E). When the platelets were pre-incubated with XO and hypoxanthine for 30 min prior to hemin addition, platelet activation was reduced almost to baseline levels of activation (16%). Febuxostat partially restored hemin-induced platelet activation with 45% of platelets being activated (Fig. 5D–E). Integration of the mean fluorescent intensity areas for the $CD41a^{+}CD62p^{+}$ platelets showed similar results (Supplemental Fig. 4B). Platelet aggregation was measured in a similar manner and calculated based on the area under the curve (AUC). Platelets were treated with ristocetin as a positive control, which showed comparable levels of platelet aggregation as hemin (Fig. 5F). Pre-incubation of platelets with XO and hypoxanthine for 30 min prior to hemin addition completely prevented platelet aggregation whereas addition of febuxostat to the reaction mixture restored hemin's ability to induce platelet aggregation (Fig. 5F).

4. Discussion

It has been well established that XO activity is elevated in numerous hemolytic conditions; however, the role of XO during hemin crisis has

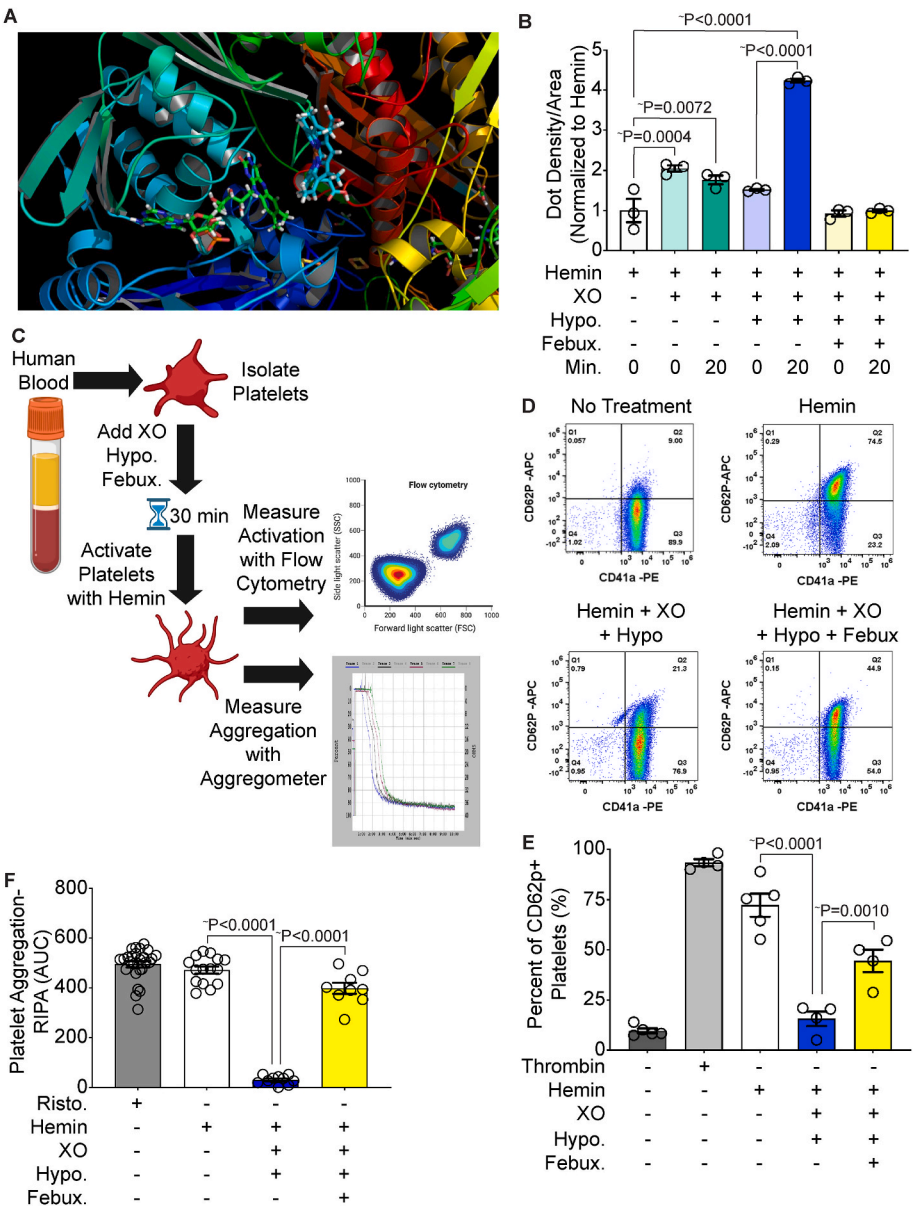

Fig. 5. XO binds hemin and prevents platelet activation and aggregation. A) Molecular modeling of hemin and XO identified a predicted hemin binding site within the FAD domain of XO. **B)** Hemin-XO interaction was evaluated via a hemin binding dot blot. Reactions were incubated for 20 min and stopped with Laemelli buffer. Samples were added to a nitrocellulose dot blot and chemiluminescent detection was used to identify hemin binding. **C)** Schematic of platelet activation and aggregation experiments. Platelets were isolated from healthy human blood and incubated with XO, hypoxanthine and febuxostat for 30 min prior to stimulation with hemin. Platelet activation was measured using flow cytometry and platelet aggregation was measured using an aggregometer. This schematic was created using biorender.com. **D-E)** Platelets were stained with the platelet marker CD41a and the platelet activation marker CD62p to determine the percentage of activated platelets in the sample. Untreated platelets were used as a negative control and thrombin was used as a positive control. Quantification of the flow scatter plots in D are shown in E. **F)** Platelet aggregation was measured using an aggregometer and calculated as the AUC. Ristocetin was used as a positive control. ~Values are mean ± SEM using a 1-way ANOVA with Sidak's multiple comparisons test. XO, xanthine oxidase; Hypo, hypoxanthine; Febux, febuxostat; Min, minute; RIPA, ristocetin-induced platelet activation; AUC, area under the curve; Risto, ristocetin.

not been experimentally defined but, rather assumed to be deleterious [21]. Hemolytic conditions, such as SCD, affect ~300,000 new patients each year [1]; however, treatment options remain limited and there are currently no SCD treatments designed specifically to target hemolysis during hemin crisis. XO has traditionally been considered a harmful enzyme when elevated during pathological conditions; however, we hypothesized that the robust increase in XO activity associated with hemolytic disease may have an important and protective role.

Healthy RBC lifespan is ~115 days [39], at which time the cells not processed in the spleen via macrophage ingestion and delivery may undergo hemolysis and release their hemoglobin and hemin into the circulation [8]. Haptoglobin and hemopexin bind hemoglobin and hemin, respectively, and target them to macrophages or the liver for catabolism and clearance [40,41]. Healthy individuals have a pool of haptoglobin and hemopexin sufficient to mitigate circulating free hemoglobin and hemin levels caused by the turnover of RBCs. In SCD patients, RBC lifespan is reduced to 2–21 days, dramatically increasing the degree of hemolysis compared to their healthy counterparts [42], which results in depletion and saturation of canonical degradation pathways and elevated free hemoglobin and hemin levels in the circulation. The Cooperative Study of Sickle Cell Disease reported that during a hemolytic crisis event, SCD patients can demonstrate circulating cell-free hemoglobin and hemin levels greater than 60 μM which is greater than a 10-fold increase over those values seen in health humans (less than 5 μM) [16,43].

We have previously shown that plasma XO levels are elevated (1.4-fold) in transgenic SCD mice and that 10 weeks of treatment with the XO inhibitor febuxostat decreased hemolysis and improved pulmonary vascular dysfunction indicating that this increased XO activity can contribute to the pathologic disease progression [31]. While results from this study demonstrated XO activity to be augmented in the circulation and to contribute to increased hemolysis and endothelial cell dysfunction in SCD mice: 1) this was observed in the absence of a crisis event, 2) it remains unclear how circulating XO activity is increased and 3) posits the question: might elevated circulating XO represent a protective response against a crisis event when considerable free hemoglobin and hemin overwhelm canonical scavenging pathways? As such, we hypothesized that there are dichotomous roles for XO, where it contributes to red cell hemolysis during basal SCD conditions but has a protective role during a hemin crisis event. To investigate the role of XO during a

hemolytic crisis event in SCD, we challenged WT AA and WT mice with hemin. The WT SS mice experienced a greater degree of hemolysis compared to the WT AA mice as evidenced by a significantly greater decrease in hematocrit and hemoglobin (Fig. 1C–D). Because the WT SS sickle mice have depleted hemopexin concentrations [31], it is not surprising to observe greater rates of hemolysis and hemin toxicity. However, a possible caveat to these observations is that the increase in hemolysis observed in the WT SS mice could be due to disease progression, rather than a greater extent of hemolysis in response to hemin challenge. Importantly however, the elevated levels of hemolysis in the WT SS sickle mice corresponded to an immense elevation (20-fold) in plasma XO activity in response to hemin challenge (Fig. 1E) and demonstrated a clear link between free hemin and release of XO into circulation. It is also critically important to note that the observed elevation in plasma XO levels post hemin challenge is abundantly greater than that seen in SCD mice without hemin challenge, 20-fold versus 1.4-fold, respectively.

We have previously observed that systemic diminution of XO activity by treatment of WT SS mice with the XO inhibitor febuxostat for 14 days prior to hemin challenge (40 μ/Kg) lead to diminished survival compared to untreated (no febuxostat) WT SS mice (50% (febuxostat) vs. 75% (control)) [44]. This led to our operating hypothesis herein: that during crisis, elevation in circulating XO may be protective and that the liver (hepatocytes) may be an essential source of this amplified. Hemopexin binds free hemin and targets it to the liver for hepatic catabolism and clearance [7,40]. Additionally, an abundance of XO is transcribed and translated in the liver and hepatic-derived XO accounts for more than 50% of XO found in murine circulation under basal conditions [27]. Furthermore, XO is noted to be released, presumably from hepatocytes to the circulation in the absence of overt liver damage (no alteration in plasma LDH and AST) where it can bind to distal endothelium via electrostatic interactions with GAGs, heparan sulfate (HS) and chondroitin sulfate (CS) [26,45–47]. This allows for an increase in XO concentration on the endothelial surface of organs that do not typically demonstrate robust XO expression. However, the mechanisms underpinning this process remain to be defined (*e.g.* mechanism of export, requisite signaling, *etc.*). Since there is: 1) an established connection between hemolytic disease and elevated circulating XO activity and 2) other pathologic processes lead to elevated circulating XO that is sequestered on the vascular endothelium, we hypothesized that the liver (hepatocytes) may be the source of elevated plasma levels of XO seen in Fig. 1E. Therefore, we tested the effects of depleting XO, specifically from the hepatocytes, on survival post hemin challenge. We transplanted SS sickle Townes bone marrow into litter mate control ($HXdh^{fl/fl}$) or hepatocyte-specific XOR knockout mice ($HXdh^{-/-}$) and challenged the mice with 40 μmol/kg of hemin (Fig. 2A). Hepatocyte-specific XO knockout was lethal post hemin challenge compared to the littermate controls, highlighting the importance of hepatic-derived XO in the response to hemin crisis and suggesting XO could be playing a protective role during hemin crisis. To our knowledge, this is the first evidence demonstrating elevated circulating XO activity may have a previously undiscovered, protective function in this context.

Despite the established connection between hemolytic disease and elevated XO activity, the mechanism of hepatic XO release has not been defined. Hemin is a known agonist of TLR4; therefore, we used siRNA knockdown and pharmacologic inhibition of TLR4 to assess the impact on XO release. Both approaches completely blunted the release of XO into the media (Fig. 3). As such, we have demonstrated for the first time, a direct link between hemin-TLR4 signaling and hepatocellular release of XO. Additionally, the release of XO seems to be specific to hemin as oxyhemoglobin did not mediate release of XO from AML12 cells. In addition, Hemin-TLR4 signaling also increased the transcription and translation of XDH and thus we hypothesize that hemin-hemopexin delivery to the liver serves as a signaling mechanism allowing hemin to bind TLR4, resulting in the downstream upregulation of hepatic XDH, release from the cells and subsequent increase in circulating XO. Whereas activation of TLR4 can elicit a number of pathways, of which some are deleterious whereas some are beneficial, targeting downstream responses of TLR4 such as activation of XOR may be a better strategy for therapeutic endeavors.

Hemolysis releases hemin and hemoglobin into circulation; therefore, we investigated the effects of XO activity on hemoglobin degradation. When incubating oxyhemoglobin with XO and xanthine, there was an obvious degradation of oxyhemoglobin. It has been previously reported that H_2O_2 can generate ferryl-hemoglobin and $O_2^{\bullet-}$ when reacting with oxyhemoglobin whereby the $O_2^{\bullet-}$ breaks the pyrrole ring in a "splitting" reaction [48,49]. EPR experiments revealed that incubation of oxyhemoglobin with XO + xanthine resulted in a significant increase in ascorbate radical production indicating the presence of free or heme-bound ferric iron (Fig. 4) [50]. Further validating XO-mediated damage to oxyhemoglobin was our observed diminished capacity of oxyhemoglobin to consume NO. NO is a vital signaling molecule in neuronal, immune, and inflammatory responses [51]; therefore, preventing hemoglobin from scavenging NO has many implications. For example, decreased NO bioactivity is a major contributing factor to complications in SCD such as pulmonary hypertension, leg ulceration, priapism, and stroke [15]. As such, the extent of XO-mediated protection during hemolytic conditions such as SCD may be amplified via increasing NO bioavailability.

Considering the discussion above regarding XO-mediated degradation of hemoglobin, we anticipated the potential for XO to also react with and potentially degrade hemin to help manage hemin overload when canonical mechanisms such as hemopexin become saturated. Molecular modeling identified a predicted hemin binding site in the FAD domain of XO (Fig. 5). We confirmed hemin-XO interaction with a hemin-binding dot blot and determined that XO turnover with xanthine enhances this interaction. Importantly, the XO-hemin binding was stronger than hemin-albumin (Supplemental Fig. 4A) which serves to validate the potential biological relevance of XO's ability to scavenge hemin. For example, the affinity for hemin-XO predicted at ~0.128 μM will robustly compete with hemin-albumin binding (K_d = 40 μM) to ensure a significant impact on protection. Confidence for the capacity of hemin to favor XO binding over albumin is reinforced by: 1) published affinity calculations were derived from studies with native albumin in the absence of fatty acids: molecules that could mask or block the binding site for hemin, 2) albumin has only one reported hemin binding site, and 3) relative concentrations of hemin in SCD crisis can potentially reach 1–2 mM whereas albumin concentrations are ~500 μM[38]. In addition, it is important to recognize that while purine-driven XO-mediated degradation of hemoglobin and potentially hemin would generate redox active Fe (e.g. "free Fe" and porphyrin complexed Fe), this process also produces uric acid. Uric acid can chelate free and some bound iron (uric acid-Fe-uric acid) to diminish its redox potential and thus diminish the potential for Fe-mediated reactions that alter cell signaling and/or induce overt damage [32]. As such, XO could be seen to provide the oxidative mechanism to degrade hemoglobin and potentially, hemin as well as the antioxidant to "mop up" excess iron.

Hemolytic diseases, including SCD, are often associated with platelet activation and reports indicate a correlation between markers of hemolysis in SCD and platelet activation [52,53]. Therefore, we evaluated the impact of hemin-XO interaction on platelet activation and aggregation. Pre-incubation of isolated healthy human platelets with XO and xanthine for 30 min, prior to stimulation with hemin, inhibited hemin-induced platelet activation and aggregation. These effects were reversible with the addition of the XO inhibitor, febuxostat (Fig. 5D–F). This suggests that an increase in XO activity in SCD crisis could help to reduce coagulation caused by elevated free hemin. Additionally, it has been reported that heparan-sulfate and chondroitin-sulfate are found on the platelet surface [54,55] which begs the question: might XO bind directly to the platelet surface to provide protection against hemin-induced platelet activation and aggregation?

While we have clearly demonstrated that hepatocellular-derived XO serves a protective role during intravascular hemin crisis in a sickle cell mouse model, there are considerable limitations to our study that serve to incentivize future work. For example, future work must include establishing a temporal relationship between the time of hemin challenge and death so that we can harvest tissue and plasma to: 1) document the circulating XO levels in the liver-specific knockout mice, 2) examine tissues for pathologic outcomes and 3) interrogate the vasculature to confirm elevation of XO on the endothelium. In addition, experiments herein describing XO-hemin binding, while indicative of strong interaction, must be further defined by detailed biochemical binding studies as well as experiments with cultured endothelial cells to demonstrate not only binding but protection against hemin challenge. Furthermore, we plan to further characterize the potential for uric acid to contribute to a salutary process. We fully acknowledge that these shortcomings are manifest in this study; however, we believe the observation of the ultimate assessment of a protective outcome, survival is important to report especially in the context of the biochemical analysis demonstrating key reactions that may contribute to a protective function for XO as well as initial insights to signaling mechanisms driving release of XO from hepatocytes.

When taken together, our previous reporting that systemic pharmacologic inhibition of XO diminishes survival in WT SS mice subjected to hemin crisis and the data herein support the conclusion that intravascular hemin challenge evokes an immense elevation in circulating XO derived from hepatocellular sources and this response is protective. These data also serve to incentivize further exploration into the signaling and biochemical mechanisms driving this process as well as more clear examination of what, where and when regarding the details of protection.

Sources of funding

This work was supported, in whole or in part, by National Institutes of Health Grants: F31 HL149241 (H. M. Schmidt); R25 HL128640 (K.C. Wood); K01 HL133331, R03 HL157878 and R56 AI165479 (D.A. Vitturi); National Institutes of Health (NIH) R01 DK124510-01 and American Heart Association 19TPA34850089 (E.E. Kelley); and R01 HL153532, R35 HL161177 and 19EIA34770095 American Heart Association Established Investigator Award (A.C. Straub). D.A. Vitturi acknowledges support from the Vascular Medicine Institute, the Hemophilia Center of Western Pennsylvania and a pilot award from National Institutes of Health grant P30 DK079307. Graphical design was provided by Anita Impagliazzo.

Declaration of competing interest

The authors declare that they have no known competing financial interests or personal relationships that could have appeared to influence the work reported in this paper.

Data availability

Data will be made available on request.

Appendix A. Supplementary data

Supplementary data to this article can be found online at https://doi.org/10.1016/j.redox.2023.102636.

References

[1] V.M. Pinto, M. Balocco, S. Quintino, G.L. Forni, Sickle cell disease: a review for the internist, Intern Emerg Med 14 (2019) 1051–1064, https://doi.org/10.1007/s11739-019-02160-x.
[2] M.D.S. Boakye, C.J. Owek, E. Oluoch, J. Wachira, Y.A. Afrane, Challenges of achieving sustainable community health services for community case management of malaria, BMC Publ. Health 18 (2018) 1150, https://doi.org/10.1186/s12889-018-6040-2.
[3] S. Dugani, J. Veillard, N. Kissoon, Reducing the global burden of sepsis, CMAJ (Can. Med. Assoc. J.) 189 (2017) E2–E3, https://doi.org/10.1503/cmaj.160798.
[4] C. Fleischmann, et al., Assessment of global incidence and mortality of hospital-treated sepsis. Current estimates and limitations, Am. J. Respir. Crit. Care Med. 193 (2016) 259–272, https://doi.org/10.1164/rccm.201504-0781OC.
[5] S.J. Head, M. Milojevic, D.P. Taggart, J.D. Puskas, Current practice of state-of-the-art surgical coronary revascularization, Circulation 136 (2017) 1331–1345, https://doi.org/10.1161/CIRCULATIONAHA.116.022572.
[6] O. Aubert, et al., COVID-19 pandemic and worldwide organ transplantation: a population-based study, Lancet Public Health 6 (2021) e709–e719, https://doi.org/10.1016/S2468-2667(21)00200-0.
[7] A. Smith, R.J. McCulloh, Hemopexin and haptoglobin: allies against heme toxicity from hemoglobin not contenders, Front. Physiol. 6 (2015) 187, https://doi.org/10.3389/fphys.2015.00187.
[8] H.M. Schmidt, E.E. Kelley, A.C. Straub, The impact of xanthine oxidase (XO) on hemolytic diseases, Redox Biol. 21 (2019), 101072, https://doi.org/10.1016/j.redox.2018.101072.
[9] S. Janciauskiene, V. Vijayan, S. Immenschuh, TLR4 signaling by heme and the role of heme-binding blood proteins, Front. Immunol. 11 (1964), https://doi.org/10.3389/fimmu.2020.01964, 2020.
[10] D.C. Rees, T.N. Williams, M.T. Gladwin, Sickle-cell disease, Lancet 376 (2010) 2018–2031, https://doi.org/10.1016/S0140-6736(10)61029-X.
[11] D.J. Weatherall, The inherited diseases of hemoglobin are an emerging global health burden, Blood 115 (2010) 4331–4336, https://doi.org/10.1182/blood-2010-01-251348.
[12] R.P. Hebbel, W.T. Morgan, J.W. Eaton, B.E. Hedlund, Accelerated autoxidation and heme loss due to instability of sickle hemoglobin, Proc. Natl. Acad. Sci. U.S.A. 85 (1988) 237–241, https://doi.org/10.1073/pnas.85.1.237.
[13] V. Jeney, et al., Pro-oxidant and cytotoxic effects of circulating heme, Blood 100 (2002) 879–887, https://doi.org/10.1182/blood.v100.3.879.
[14] S.C. Liu, S. Zhai, J. Palek, Detection of hemin release during hemoglobin S denaturation, Blood 71 (1988) 1755–1758.
[15] M.T. Gladwin, E. Vichinsky, Pulmonary complications of sickle cell disease, N. Engl. J. Med. 359 (2008) 2254–2265, https://doi.org/10.1056/NEJMra0804411.
[16] E.P. Vichinsky, et al., Acute chest syndrome in sickle cell disease: clinical presentation and course. Cooperative Study of Sickle Cell Disease, Blood 89 (1997) 1787–1792.
[17] U. Muller-Eberhard, J. Javid, H.H. Liem, A. Hanstein, M. Hanna, Plasma concentrations of hemopexin, haptoglobin and heme in patients with various hemolytic diseases, Blood 32 (1968) 811–815.
[18] R.D. Wochner, I. Spilberg, A. Iio, H.H. Liem, U. Muller-Eberhard, Hemopexin metabolism in sickle-cell disease, porphyrias and control subjects–effects of heme injection, N. Engl. J. Med. 290 (1974) 822–826, https://doi.org/10.1056/NEJM197404112901503.
[19] O.A. Adisa, et al., Association between plasma free haem and incidence of vaso-occlusive episodes and acute chest syndrome in children with sickle cell disease, Br. J. Haematol. 162 (2013) 702–705, https://doi.org/10.1111/bjh.12445.
[20] J.R. Delanghe, M. R. Hemopexin Langlois, A review of biological aspects and the role in laboratory medicine, Clin. Chim. Acta 312 (2001) 13–23, https://doi.org/10.1016/s0009-8981(01)00586-1.
[21] M. Aslan, et al., Oxygen radical inhibition of nitric oxide-dependent vascular function in sickle cell disease, Proc. Natl. Acad. Sci. U.S.A. 98 (2001) 15215–15220, https://doi.org/10.1073/pnas.221292098.
[22] U.R. Osarogiagbon, et al., Reperfusion injury pathophysiology in sickle transgenic mice, Blood 96 (2000) 314–320.
[23] K.A. Pritchard Jr., et al., Hypoxia-induced acute lung injury in murine models of sickle cell disease, Am. J. Physiol. Lung Cell Mol. Physiol. 286 (2004) L705–L714, https://doi.org/10.1152/ajplung.00288.2002.
[24] P. Pacher, A. Nivorozhkin, C. Szabo, Therapeutic effects of xanthine oxidase inhibitors: renaissance half a century after the discovery of allopurinol, Pharmacol. Rev. 58 (2006) 87–114, https://doi.org/10.1124/pr.58.1.6.
[25] J. Sikora, S.N. Orlov, K. Furuya, R. Grygorczyk, Hemolysis is a primary ATP-release mechanism in human erythrocytes, Blood 124 (2014) 2150–2157, https://doi.org/10.1182/blood-2014-05-572024.
[26] M. Houston, et al., Binding of xanthine oxidase to vascular endothelium. Kinetic characterization and oxidative impairment of nitric oxide-dependent signaling, J. Biol. Chem. 274 (1999) 4985–4994, https://doi.org/10.1074/jbc.274.8.4985.
[27] D.B. Harmon, et al., Hepatocyte-specific ablation or whole-body inhibition of xanthine oxidoreductase in mice corrects obesity-induced systemic hyperuricemia without improving metabolic abnormalities, Diabetes 68 (2019) 1221–1229, https://doi.org/10.2337/db18-1198.
[28] B.J. O'Donnell, et al., Sleep phenotype in the Townes mouse model of sickle cell disease, Sleep Breath. 23 (2019) 333–339, https://doi.org/10.1007/s11325-018-1711-x.
[29] T.M. Ryan, D.J. Ciavatta, T.M. Townes, Knockout-transgenic mouse model of sickle cell disease, Science (New York, N.Y.) 278 (1997) 873–876, https://doi.org/10.1126/science.278.5339.873.
[30] K.C. Wood, et al., Smooth muscle cytochrome b5 reductase 3 deficiency accelerates pulmonary hypertension development in sickle cell mice, Blood Adv. 3 (2019) 4104–4116, https://doi.org/10.1182/bloodadvances.2019000621.
[31] H.M. Schmidt, et al., Xanthine oxidase drives hemolysis and vascular malfunction in sickle cell disease, Arterioscler. Thromb. Vasc. Biol. 41 (2021) 769–782, https://doi.org/10.1161/ATVBAHA.120.315081.

[32] K.J. Davies, A. Sevanian, S.F. Muakkassah-Kelly, P. Hochstein, Uric acid-iron ion complexes. A new aspect of the antioxidant functions of uric acid, Biochem. J. 235 (1986) 747–754, https://doi.org/10.1042/bj2350747.
[33] E.E. Kelley, G.R. Buettner, C.P. Burns, Production of lipid-derived free radicals in L1210 murine leukemia cells is an early oxidative event in the photodynamic action of Photofrin, Photochem. Photobiol. 65 (1997) 576–580, https://doi.org/10.1111/j.1751-1097.1997.tb08608.x.
[34] A.C. Straub, et al., Endothelial cell expression of haemoglobin alpha regulates nitric oxide signalling, Nature 491 (2012) 473–477, https://doi.org/10.1038/nature11626.
[35] S. Ghosh, et al., Extracellular hemin crisis triggers acute chest syndrome in sickle mice, J. Clin. Invest. 123 (2013) 4809–4820, https://doi.org/10.1172/JCI64578.
[36] C. Helms, D.B. Kim-Shapiro, Hemoglobin-mediated nitric oxide signaling, Free Radic. Biol. Med. 61 (2013) 464–472, https://doi.org/10.1016/j.freeradbiomed.2013.04.028.
[37] J. Rozga, T. Piatek, P. Malkowski, Human albumin: old, new, and emerging applications, Ann. Transplant. 18 (2013) 205–217, https://doi.org/10.12659/AOT.889188.
[38] J.K. Kamal, D.V. Behere, Binding of heme to human serum albumin: steady-state fluorescence, circular dichroism and optical difference spectroscopic studies, Indian J. Biochem. Biophys. 42 (2005) 7–12.
[39] R.S. Franco, Measurement of red cell lifespan and aging, Transfus. Med. Hemother. 39 (2012) 302–307, https://doi.org/10.1159/000342232.
[40] F. Vinchi, et al., Hemopexin therapy reverts heme-induced proinflammatory phenotypic switching of macrophages in a mouse model of sickle cell disease, Blood 127 (2016) 473–486, https://doi.org/10.1182/blood-2015-08-663245.
[41] M.D. Jain, et al., Seek and you shall find–but then what do you do? Cold agglutinins in cardiopulmonary bypass and a single-center experience with cold agglutinin screening before cardiac surgery, Transfus. Med. Rev. 27 (2013) 65–73, https://doi.org/10.1016/j.tmrv.2012.12.001.
[42] M.H. Steinberg, Sickle cell anemia, the first molecular disease: overview of molecular etiology, pathophysiology, and therapeutic approaches, Sci. World J. 8 (2008) 1295–1324, https://doi.org/10.1100/tsw.2008.157.
[43] J.Y. Oh, et al., Absorbance and redox based approaches for measuring free heme and free hemoglobin in biological matrices, Redox Biol. 9 (2016) 167–177, https://doi.org/10.1016/j.redox.2016.08.003.
[44] H. Schmidt, S. Hahn, G. Annarapu, M. Carreno, K. Wood, S. Shiva, D. Vitturi, E. Kelley, A. Straub, Xanthine oxidase has a protective role during heme crisis by binding heme and facilitating degradation, Free Radic. Biol. Med. 180 (2022) 53, https://doi.org/10.1016/j.freeradbiomed.2021.12.118.
[45] R. Radi, H. Rubbo, K. Bush, B.A. Freeman, Xanthine oxidase binding to glycosaminoglycans: kinetics and superoxide dismutase interactions of immobilized xanthine oxidase-heparin complexes, Arch. Biochem. Biophys. 339 (1997) 125–135, https://doi.org/10.1006/abbi.1996.9844.
[46] T. Fukushima, T. Adachi, K. Hirano, The heparin-binding site of human xanthine oxidase, Biol. Pharm. Bull. 18 (1995) 156–158, https://doi.org/10.1248/bpb.18.156.
[47] S. Tan, et al., Xanthine oxidase activity in the circulation of rats following hemorrhagic shock, Free Radic. Biol. Med. 15 (1993) 407–414, https://doi.org/10.1016/0891-5849(93)90040-2.
[48] J.M. Rifkind, E. Nagababu, S. Ramasamy, L.B. Ravi, Hemoglobin redox reactions and oxidative stress, Redox Rep. 8 (2003) 234–237, https://doi.org/10.1179/135100003225002817.
[49] E. Nagababu, J.M. Rifkind, Reaction of hydrogen peroxide with ferrylhemoglobin: superoxide production and heme degradation, Biochemistry 39 (2000) 12503–12511, https://doi.org/10.1021/bi992170y.
[50] G.R. Buettner, B.A. Jurkiewicz, Ascorbate free radical as a marker of oxidative stress: an EPR study, Free Radic. Biol. Med. 14 (1993) 49–55, https://doi.org/10.1016/0891-5849(93)90508-r.
[51] N. Tuteja, M. Chandra, R. Tuteja, M.K. Misra, Nitric oxide as a unique bioactive signaling messenger in physiology and pathophysiology, J. Biomed. Biotechnol. (2004) 227–237, https://doi.org/10.1155/S1110724304402034, 2004.
[52] C.C. Helms, et al., Mechanisms of hemolysis-associated platelet activation, J. Thromb. Haemostasis 11 (2013) 2148–2154, https://doi.org/10.1111/jth.12422.
[53] J. Villagra, et al., Platelet activation in patients with sickle disease, hemolysis-associated pulmonary hypertension, and nitric oxide scavenging by cell-free hemoglobin, Blood 110 (2007) 2166–2172, https://doi.org/10.1182/blood-2006-12-061697.
[54] O.A. Hamad, et al., Contribution of chondroitin sulfate A to the binding of complement proteins to activated platelets, PLoS One 5 (2010), e12889, https://doi.org/10.1371/journal.pone.0012889.
[55] H.B. Nader, Characterization of a heparan sulfate and a peculiar chondroitin 4-sulfate proteoglycan from platelets. Inhibition of the aggregation process by platelet chondroitin sulfate proteoglycan, J. Biol. Chem. 266 (1991) 10518–10523.